Stanford Exploration Project, Report 110, September 18, 2001, pages 1–162

Short Note

AVA attributes (2 for 1 special)

Brad Artman[1]

INTRODUCTION

Once satisfied that an amplitude, as produced by the user's favorite migration process/algorithm, contains sufficiently accurate and interesting information, the use of that knowledge must be simple and enlightening. Herein I will introduce an AVA (or O if you insist) attribute that is easily calculated, quickly interpreted, and physically meaningful. This attribute will be derived from a different, though related, cross-plot that shows significant improvement over the classic *Intercept-Gradient* plane.

While it is clear that there are likely few geophysicists truly excited about the introduction of yet another seismic attribute, I believe that Shale-Normal Amplitude (SNA) analysis described herein can greatly ease and quantify the interpretation of AVA data. The premise is very simple and the output concise and enlightening. The attribute is derived from a *Compression-PseudoShear* reflection coefficient plane that allows significantly more insight into the lithologies at depth than the traditional *Intercept-Gradient* $(A-B)$ plane.

THE PSEUDO-SHEAR REFLECTION COEFFICIENT

Most practitioners are by now familiar with $A-B$ plots for AVA analysis. The SNA attribute operates on a permutation of the $A-B$ plane described below. The Zoeppritz equation approximation for small physical contrasts over intermediate angles presented by Shuey (1985) is:

$$R(\theta) \approx A + B\sin^2\theta \,, \tag{1}$$

where

$$A = \frac{\Delta\rho}{2\rho+\Delta\rho} + \frac{\Delta V_p}{2V_p+\Delta V_p} \tag{2}$$

and

$$B = A - 2C \,,$$

[1]**email:** brad@sep.stanford.edu

with C having the form

$$C = \frac{1+\eta}{2}\,\frac{\Delta\rho}{2\rho+\Delta\rho} + \eta\frac{\Delta V_s}{2V_s+\Delta V_s} \tag{3}$$

where

$$\eta = 4\frac{V_s^2}{V_p^2}\,.$$

Δ quantities are the differences layer 1 minus layer 2. Density and velocities (without Δ) are those of layer 2. Also, I have reordered the usual relationship to lead the reader toward the goal of orthogonalizing the AVA plane between compressional and shear axes. With the above development of the Shuey equation, we see A is the normal incidence compressional reflection amplitude and B contains both normal incidence and angular dependence. Other authors, such as Castagna et al. (1998), have attempted to simplify this relationship by expressing B as a complicated function of A multiplied by new (empirical) fitting coefficients. While facilitating ever more cross-plotting possibilities, axes remain mixtures of compressional and shear quantities and yield little more insight.

However, with the above formulation of Shuey equation (1) we can separate B into the compressional, A, and *pseudo*-shear, C, reflection amplitude coefficients. Notice the very parallel structure of the *pseudo*-shear, equation 3, to the normal incidence term, equation 2, and its independence from compressional velocity contrast. Encouragingly, the *pseudo*-shear expression contracts to the normal incidence shear reflection coefficient when the compressional to shear velocity ratio γ equals 2.

This separation (effectively between $A(\Delta V_p)$ and $C(\Delta V_s)$) will help guide our intuition by isolating the seismic reflection amplitude into two components that have meaning in an AVA sense. Rather than plotting on the $A-B$ plane, we can utilize the $A-C$ plane and avoid an ordinate with codependency of compressional and shear velocity boundary contrasts.

With the insight gained from the definitions of A and C, we can now intuitively understand that trends in this AVA plane are due to the variation of real rock properties. **Figure 1** indicates the relative position of simple targets in this space. Because I have defined density and velocity as the properties of the lower layer, the negative values of A show a change from harder to softer intervals and the opposite is true for the positive values. Therefore we can understand something of the nature of the bounding layers of an interval as harder bounding lithologies will trend to more negative values of A.

We also know that the shear velocity of a porous medium increases as we lower the density of the included fluid. This tells us that the ΔV_s will be negative as we consider a water filled medium versus a gas filled one and this will increasingly drive the value of C more negative. The interplay between these compressional and shear forces results in the normal NW-SE trend of the data cloud in **Figure 1** indicating hard bounding rocks upward and soft ones downward.

Gratwick (2001b) outlined the promise and difficulty of prospecting AVA anomalies on an $A-B$ plane as explained by Castagna and Swan (1997). Both authors stress the importance of the distance away from the background trend for the analysis of a prospective event. Attempting to quantify this, Gratwick (2001b) calculates the product of A with B, then masks the cen-

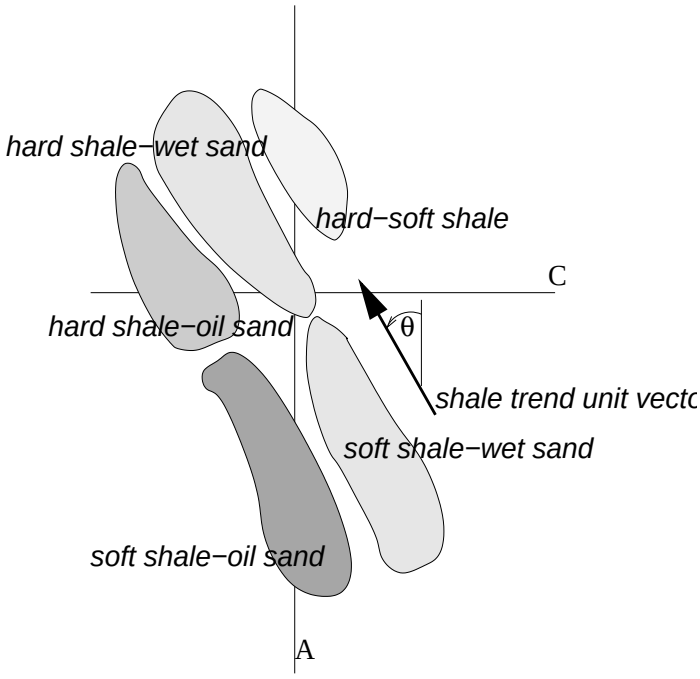

Figure 1: With the clarity of structure of equation (3) for C, simple test case plots can be readily manufactured by applying it to mental scenarios within this cartoon. brad2-cartoon [NR]

ter mass of reflection amplitudes that are assumed to be background values (non-prospective shale-wet sand or shale-shale reflections). This process is shown in **Figure 2**. The flaw in this method is the dull spoon that differentiates anomalies from background. Not only is the scalpel dull, but this methodology only appreciates a single model type. More practically, the clumsy transfer in and out of SEP architecture for graphical definition of the mute zone can dissuade all but the most committed from utilizing this tool.

Figure 3 (*i*) shows the standard Slope-Intercept AVA plot, while **(*ii*)** shows the transform to the Compressional-PseudoShear plane. The data are generated from a synthetic provided by BP and explained in detail by Gratwick (2001b). While immediately displeasing, these two plots will highlight the power of the $A-C$ plane when inspected. First note the strong zero presence on the intercept-axis of the $A-B$ panel. This is modeled data, boring, and makes our unit vector for the shale trend very simple ($\theta = 0$). In an attempt to provide a small measure of believable scatter (make this plot less boring), a bandpass filter was run over the AVA attributes. [2] This contributes to a few bothersome artifacts, but are easy to neglect. These include: data present to the left of shale trend (bandpassing 0 returns negative values), diagonal sub-trends of events, and incomplete orthogonalization. We see that due to the presence of both shear and compressional velocity contrasts in the formulation of B, the transition of reflections on the $A-B$ plot from water to oil to gas takes place along a line with an acute angle to the background trend. This leads to one of the paramount problems with interpreting AVA anomalies as explained in Castagna (1997). The $A-C$ plane, enjoying an ordinate quantity that is a function only of a change across the boundary of the shear velocity, shows nice perpendicular [3] departure from the axis of the compressional reflection coefficient.

[2] Without such, only four points are seen on the plane.

[3] I really think it would be without the bandpass issues

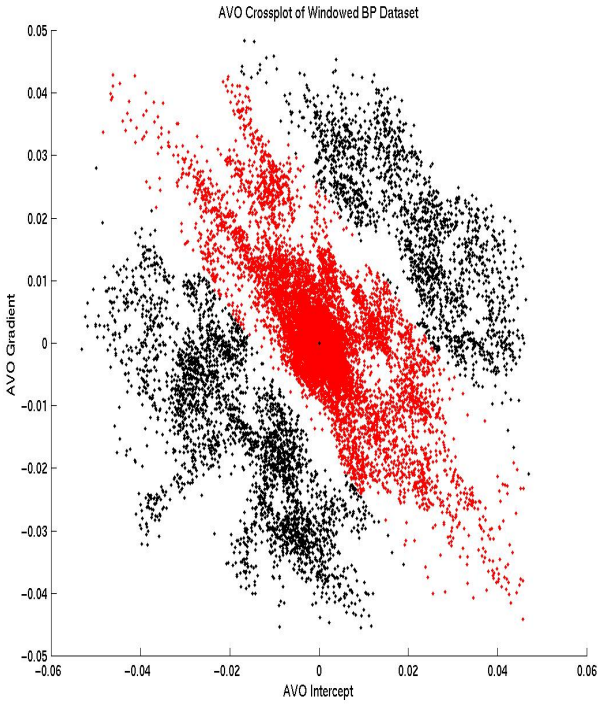

Figure 2: A vs. B scatter-plot with mute fairway defined. Gratwick (2001b) brad2-plot2 [NR]

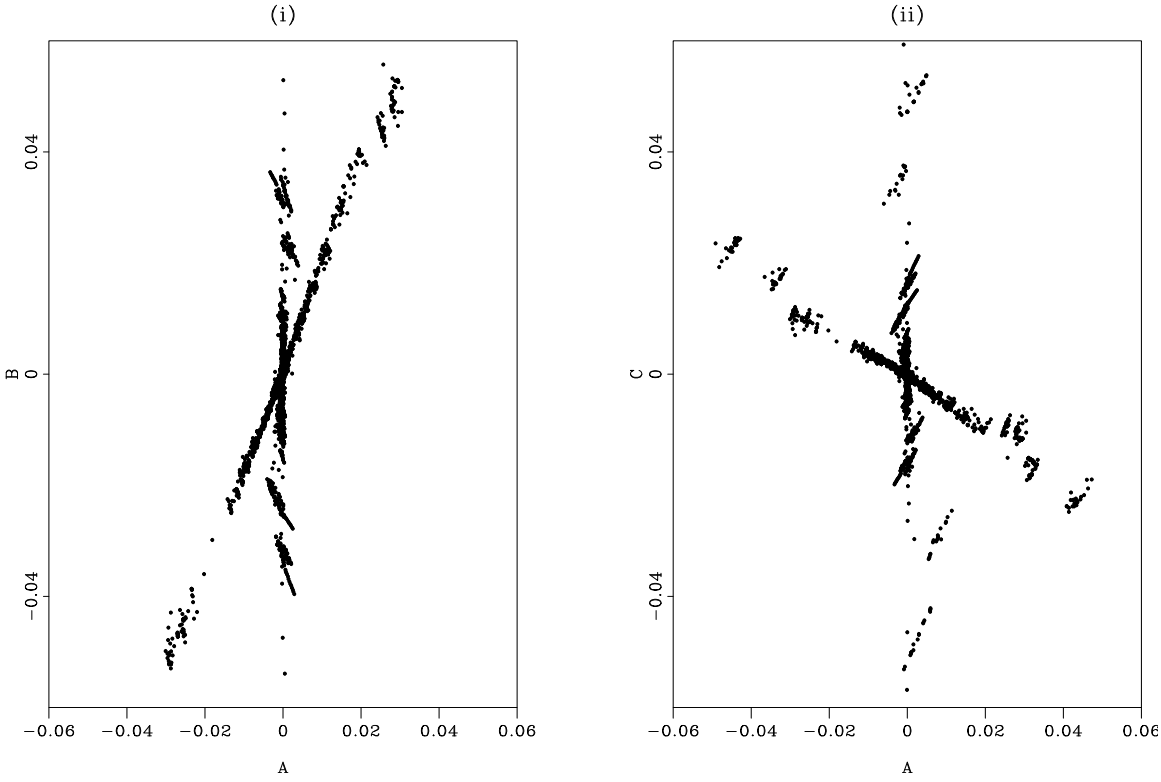

Figure 3: The ordinate axis is transformed from B, Shuey's gradient, to compressional the pseudo-shear reflection coefficient C. brad2-planes [ER,M]

SHALE-TREND NORMAL AMPLITUDE

Intuitively now, we have developed an understanding for where on the $A-C$ plane to expect prospective events and a little about what a location on the plane indicates about the rocks. The perpendicular distance away from the shale trend explained above is what truly quantifies an AVA anomaly. Therefore, if we can define a unit vector that accurately describes the shale trend, the cross-product with a vector containing the values of A and C for any point in the subsurface will interpret whether that point is *anomalous* or not. This quantity I will call the Shale-normal Amplitude. Simply stated, defining the reflection coefficient vector

$$\vec{RFC} = (A,C)$$

and the shale trend background vector

$$\vec{S} = (cos\theta, sin\theta)$$

the Shale-Normal Amplitude is

$$SNA = \frac{|\vec{RFC} \times \vec{S}|}{|\vec{S}|} = \frac{Asin\theta - Ccos\theta}{|\vec{S}|}. \tag{4}$$

USE AND APPLICATION

Piggy-backing directly on the development and results of (Gratwick, 2001b), and assuming that all necessary precautions in dealing with amplitudes as a function of angle have been taken into account (as detailed in (Gratwick, 2001a)), we can compare the $A*B$ mute method with the SNA analysis. Analogous with the mute method, a threshold value for the SNA will need to be selected.[4]

This value can be chosen by inspection of a SNA histogram. We can hope for clean separation of roughly Gaussian distributions of shale-wet sand reflections and shale-oil sand (and/or shale-gas sand) resulting in a bi- or tri-modal distribution of reflections. As discussed above, the less dense the pore-filling fluid, the higher the SNA value. Therefore, assuming only that most intervals are water-bearing, we can confidently pick the first mode as indicative of water reflections. **Figure 4** shows an ideal distribution of SNA, while **Figure 5** shows the histogram for the synthetic data.

An even more powerful approach is to extract the SNA attribute along an event and plot it as a function of depth or time. As the event crosses fluid levels, we will see nice step-changes in the SNA value.[5]

[4]This method is not salt-proof. Like so many other things salt really screws up things. All analysis here-in has windowed out the region of the salt body.

[5]While these well behaved model amplitudes are picked by peak amplitude, the author will freely rant upon request about the importance of using some product of amplitude and thickness of wavelet when analysing real data.

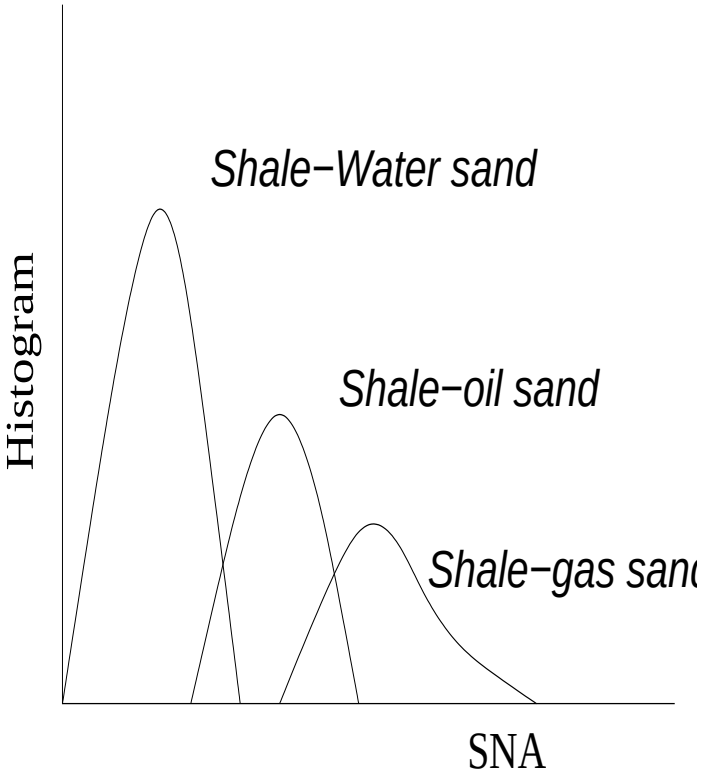

Figure 4: Ideal distributions of SNA attribute. Threshold values for color tables or clipping can be set with these in mind for fast and furious prospecting or horizon mapping and volumetrics. brad2-ideal [NR]

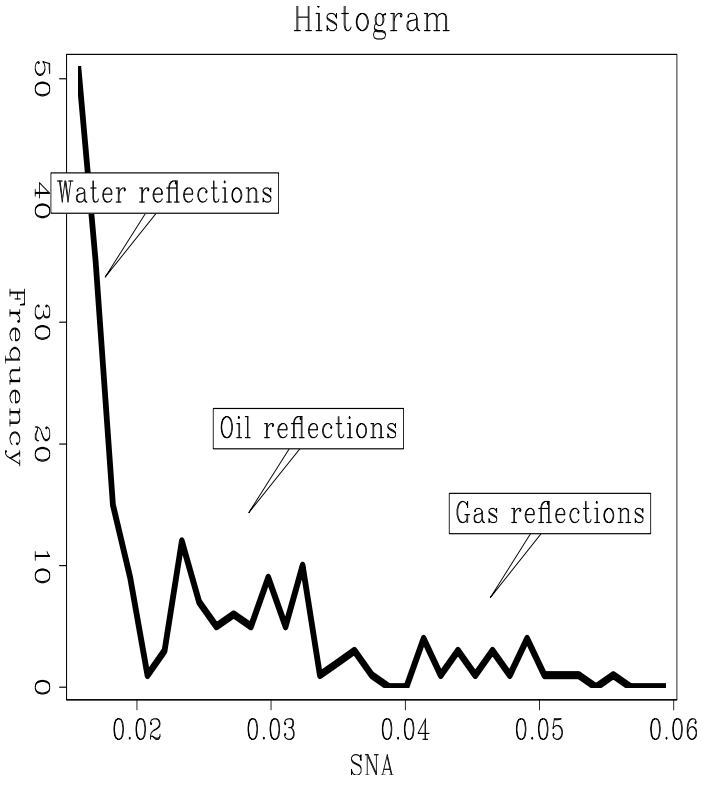

Figure 5: Histogram of SNA from modeled then migrated from the density/velocity grid shown in 6. The extreme preponderance of zero values in the model makes the plot ugly, but the tri-modal nature of the histogram is evident. brad2-histo [ER]

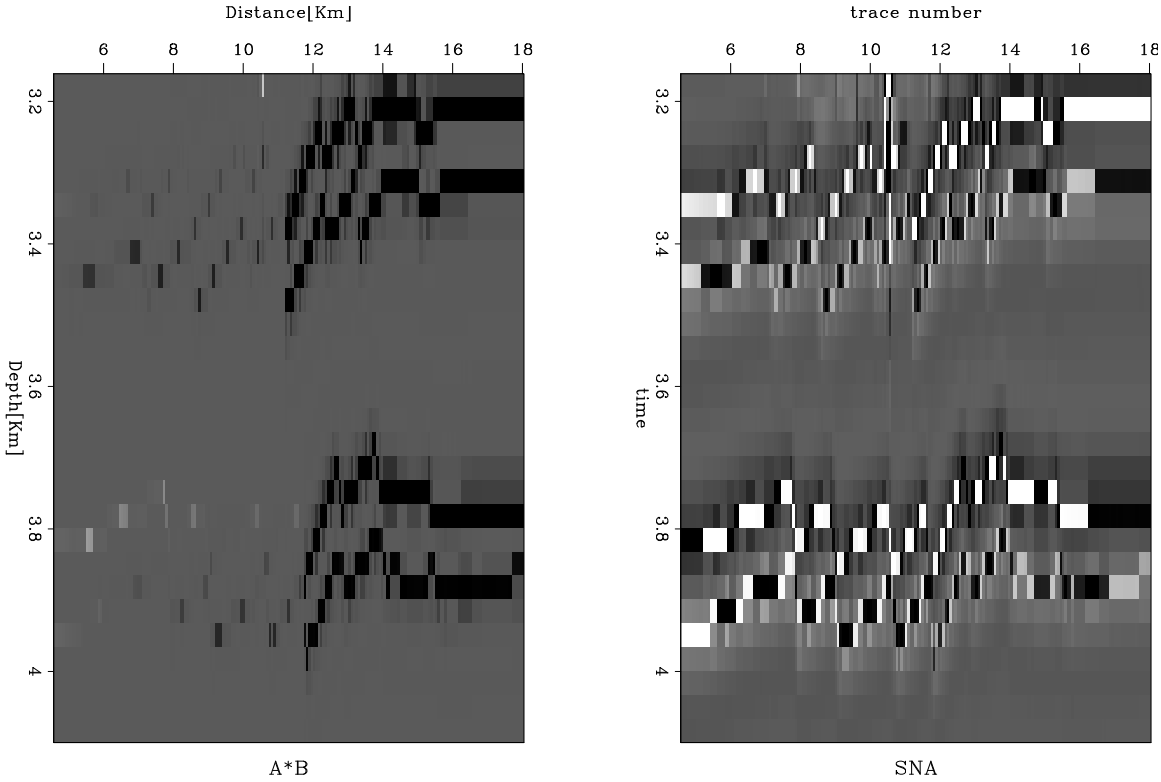

Figure 6: Zoom of "reservoirs" from V_p, V_s, and ρ models. Gratwick (2001b) shows the entire model and details the processing steps. White denotes high A*B value (down-dip water reflections have already been muted). Notice the accuracy of the SNA model showing prospective AVA character on the top reservoir reflection, but not the bottom reflection. **Figure 5** shows picks along the upper-most reflector. brad2-models [ER,M]

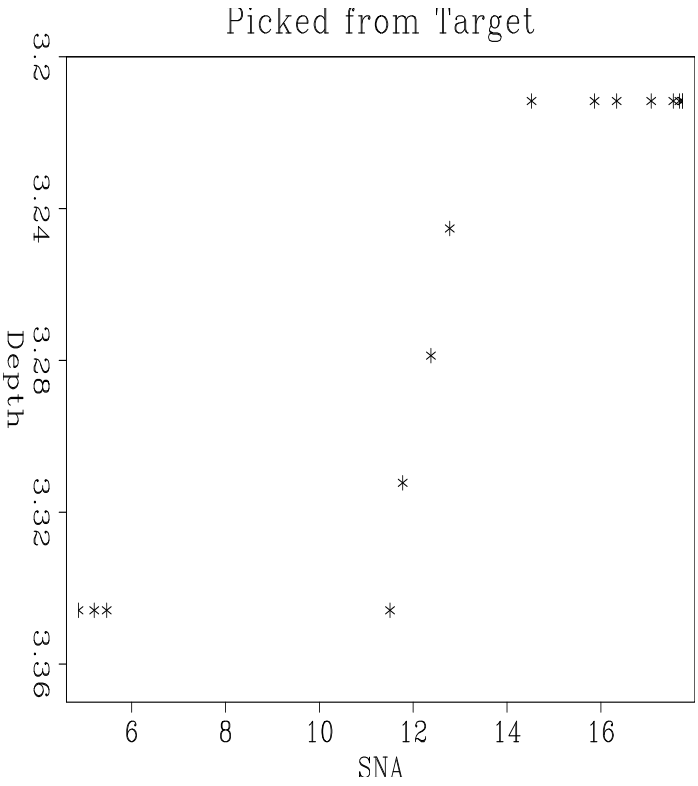

Figure 7: While fault blocks complicate the plot somewhat, fluid level remains obvious, and a prospecting threshold of 12-14 is comfortably assigned. Values were not normalized by $|\vec{S}|$. brad2-event [ER]

To use this type of analysis on well or seismic data (integration!), one is only required to perform the trivial calculations of equations (1) and/or (3) to generate the $A-C$ plane. Further, after estimating the Shale trend angle on the plot,[6] the SNA attribute can be calculated and used as a prospecting or reservoir characterization tool.

The next step in proving the value of this concept will be to apply these simple transformations to single events known to have fluid contacts. Such a data set is thought to exist in-house, and a thorough description of our success/failure with this analysis will be included in the next report.

ACKNOWLEDGMENTS

I would like to acknowledge Doug Gratwick's work in SEP108 upon which the examples used herein are built.

[6]It is unclear whether simple regression on this plane could result in incorrect unit vectors without the dismissal of anomalous points by an interpreter. What is encouraging is that in the test thus far, these calculations are very insensitive to the precision of the θ.

REFERENCES

Castagna, J. P., and Swan, H. W., 1997, Principles of AVO crossplotting: AAPG Mid-Continent Section Meeting; Abstracts; AAPG Bulletin, **81**, no. 8, 1348.

Castagna, J. P., Swan, H. W., and Foster, D. J., 1998, Framework for AVO gradient and intercept interpretation: Geophysics, **63**, no. 3, 948–956.

Gratwick, D., 2001a, The accuracy of wave-equation migration amplitudes: SEP–**108**, 63–72.

Gratwick, D., 2001b, Amplitude analysis in the angle domain: SEP–**108**, 45–62.

Shuey, R. T., 1985, A simplification of the Zoeppritz equations: Geophysics, **50**, no. 4, 609–614.